CHAPTER 8

Current-Depth Refraction and Diffraction Model for Irregular Water Waves

Jang Won Chae[1] and Shin Taek Jeong[2]

Abstract

A numerical model is presented for the prediction of combined refraction-diffraction of waves propagating in the region of slowly varying current and topography. For steady waves, two elliptic-type model equations are derived from the mild-slope equation which can be solved in a similar way to an initial value problem without stability restriction. Therefore, the present model appears to be an efficient tool for irregular wave propagation problem in a large coastal area. Some examples of numerical computations are given for the cases concerning wave-current interaction on a sloping beach and over a mound.

Introduction

Waves propagating near a tidal inlet will be transformed due to currents and irregular water depths. The wave-current interaction is one of the most interesting and important phenomena for the prediction of wave climate and resultant sediment transport in coastal areas. The approximation of irregular waves by a monochromatic wave in modeling of wave transformation in coastal areas often introduces large errors in wave heights. There is a definite need for an efficient method for the calculation of irregular wave transformation over large coastal area(Panchang et al., 1990).

[1] Principal Res. Engr., Head of Coast. Engrg. Lab., Korea Ocean Res. & Dev. Inst., Ansan P.O. Box 29, Seoul 425-600, Korea.

[2] Senior Res. Engr., Coast. Engrg. Lab., Korea Ocean Res. & Dev. Inst. Ansan P.O. Box 29, Seoul 425-600, Korea.

Recently, a number of studies have been made for the analysis of wave-current system. Booij(1981), Liu(1983), and Kirby(1984) proposed hyperbolic wave equations governing the propagation of waves in water of varying depth and currents in the mild-slope approximation. They used parabolic approximation in order to circumvent the difficulty in calculation of elliptic equations for regular waves. Ohnaka et al.(1988) provided a set of mild-slope equations based on Kirby's equation, which consists of two first-order equations describing the water surface elevation and flow rate. This model includes partially reflective boundary condition.

The models mentioned above employ parabolic- or hyperbolic-type differential equations which are in general not so efficient to use in large area (order of hundreds of wave length). In shallow water they need fine grid resolution to meet sufficient accuracy of numerical results, which is more crucial condition for the high frequency components of wave spectrum.

In the present study, a new set of mild-slope equations describing the deformation of regular waves by a large-scale current field in water of irregular depth is derived, and an efficient numerical method is also presented. The elliptic type governing equations are solved in a similar way to an initial value problem. The accuracy of the numerical method does not greatly depend on grid size and computation time is comparatively short. Therefore, this method is extensively applied to several spectral components in order to simulate irregular wave transformation due to combined refraction-diffraction. Linear superposition of monochromatic-wave calculation is made to obtain spectral estimates. Some results of the computation are compared with analytical solutions, and numerical examples concerning the interactions between waves and currents over a mildly sloping beach and also over a mound are presented.

Derivation of Governing Equations

The mild-slope equation has been used successfully as a model equation for describing surface water waves propagating over a seabed of mild slope(eg. Berkhoff, 1972). For a wave-current interaction Kirby(1984) derived a general equation. Recently Chae et al.(1990) and Jeong(1990) have rederived the mild-slope equation using variational principle and Green's theorem for linear water waves following Booij's method(1981). The equation can be written as

$$\frac{D^2\Phi}{Dt^2}+(\nabla\cdot\underline{U})\frac{D\Phi}{Dt}-\nabla\cdot(CCg\nabla\Phi)+(\sigma^2-k^2CCg)\Phi+W\frac{\partial\Phi}{\partial t}=0 \qquad (1)$$

where $D/Dt = \partial/\partial t + \underline{U}\cdot\nabla$, $\nabla = [(\partial/\partial x)\, i,\ (\partial/\partial y)\, j]$, and $\underline{U} = (u\ ,\ v)$, Φ the complex velocity potential at the mean surface level, σ the intrinsic angular frequency, k wave number, C and Cg are the phase and group velocity respectively, which are defined according to $C = \sigma/k$, $Cg = \partial\sigma/\partial k$, $\sigma^2 = gk \tanh kh$, and W dissipation coefficient,

$$\omega = \sigma + \underline{k}\cdot\underline{U} \tag{2}$$

where ω is absolute angular frequency. The velocity potential at an elevation z is given by

$$\Phi(\underline{x}, z, t) = f(z)\, \phi(\underline{x}, t) \tag{3}$$

where $f(z) = (\cosh k(z+h))/(\cosh kh)$. Since the bottom is mildly sloping, the derivative of f with respect to $\underline{x}$ will be small.

For purely periodic waves the velocity potential is given by

$$\phi(\underline{x}, t) = \mathrm{Re}\left[\hat{\phi}(\underline{x})e^{-i\omega t}\right] \tag{4}$$

Substitutions of eq.(4) into eq.(3), and further them into eq.(1) produce an elliptic equation as follows:

$$\begin{aligned} &- i\omega\left[2\underline{U}\cdot\nabla\hat{\phi} + \hat{\phi}(\nabla\cdot\underline{U})\right] + (\underline{U}\cdot\nabla)(\underline{U}\cdot\nabla\hat{\phi}) + (\nabla\cdot\underline{U})(\underline{U}\cdot\nabla\hat{\phi}) \\ &- \nabla\cdot(CCg\nabla\hat{\phi}) + (\sigma^2 - \omega^2 - k^2CCg) - i\omega W\hat{\phi} = 0 \end{aligned} \tag{5}$$

If $\underline{U} = (0, 0)$, eq.(5) reduces to Berkhoff's(1972) mild-slope equation.

Here the complex velocity potential $\hat{\phi}$ can be written in terms of the amplitude a and the phase S as

$$\hat{\phi} = -ig\frac{a}{\sigma}e^{iS} \tag{6}$$

where g is acceleration due to gravity, and $S(\underline{x})$ phase function given by

$$S(\underline{x}) = \underline{k}\cdot\underline{x} - \omega t \tag{7}$$

Then eq.(5) with the substitution of eq.(6) reduces to a set of elliptic equations by separating the resulting equation into real and imaginary parts as follows

$$\nabla\cdot\left[\underline{U}\frac{a^2}{\sigma^2}(\omega - \underline{U}\cdot\nabla S) + CCg\frac{a^2}{\sigma^2}\nabla S\right] + W\frac{a^2}{\sigma} = 0 \tag{8}$$

$$\begin{aligned} &CCg\frac{a}{\sigma}(\nabla S)^2 - (\underline{U}\cdot\nabla S - \omega)^2\frac{a}{\sigma} + (\sigma^2 - k^2CCg)\frac{a}{\sigma} \\ &- \nabla\cdot(CCg\frac{a}{\sigma}) + (\nabla\cdot\underline{U})(\underline{U}\cdot\nabla\frac{a}{\sigma}) + \underline{U}\cdot\nabla(\underline{U}\cdot\nabla\frac{a}{\sigma}) = 0 \end{aligned} \tag{9}$$

These are the final forms of the wave equation for this numerical model study. In the present paper, we are concerned with the problems where W is assumed zero for simplicity and the mean current is in the following condition

$$|\underline{U}|^2 \ll CCg \tag{10}$$

Eq.(9) then can be simplified as follows:

$$CCg\frac{a}{\sigma}(\nabla S)^2 - (\underline{U}\cdot\nabla S - \omega)^2 \frac{a}{\sigma} + (\sigma^2 - k^2 CCg)\frac{a}{\sigma} - \nabla\cdot(CCg\nabla\frac{a}{\sigma}) = 0 \tag{11}$$

If we set $\underline{U}$ = (0, 0), eqs.(8) and (11) reduce to the Ebersole's(1985) model equations for depth refraction-diffraction. Further, the equation of wave action conservation for steady waves can be simply obtained from eq.(8).

The main wave direction θ can be given from eq.(12) with the combination of eqs.(8) and (11). The irrotationality condition of wave number vector is

$$\frac{\partial(|\nabla S|\sin\theta)}{\partial x} = \frac{\partial(|\nabla S|\cos\theta)}{\partial y} \tag{12}$$

Numerical Computation

Both eqs.(8) and (11) are of the elliptic type and can generally be solved as a boundary value problem using finite element method. If we neglect wave reflections from boundaries, and also if approximate intermediate values of wave properties can be provided at all grid points using a refraction model, the problem can be converted into an initial value problem for the wave diffraction (eg. Ebersole, 1985).

Finite difference method is adopted to solve the governing equations (8), (11) and (12). The coordinate and grid systems as shown in Figure 1 are employed. Forward difference scheme is used in x-direction and centered scheme in y-direction to approximate the eq(8), which yields the following difference equations.

$$(a_j^i)^2 b_j^i = (a_j^{i+1})^2 b_j^{i+1} + \frac{\Delta x}{2\Delta y}\left[(a_{j+1}^i)^2 b_{j+1}^i - (a_{j-1}^i)^2 b_{j-1}^i\right] \tag{13}$$

where

$$b_j^i = \left(\frac{1}{\sigma^2}\right)_j^i \left[U(\omega - \underline{U}\cdot\nabla S) + CCg|\nabla S|\cos\theta + V(\omega - \underline{U}\cdot\nabla S) + CCg|\nabla S|\sin\theta\right]_j^i$$

$$(a_j^{i+1})^2 b_j^{i+1} = \tau(a_{j-1}^{i+1})^2 b_{j-1}^{i+1} + (1 - 2\tau)(a_j^{i+1})^2 b_j^{i+1} + \tau(a_{j+1}^{i+1})^2 b_{j+1}^{i+1}$$

where τ is Abbott's dissipative interface factor ($0 \le \tau \le 0.5$).

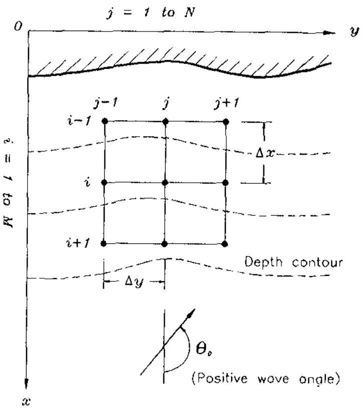

Figure 1. Definition of coordinate system, grid cell and wave angle conventions.

Eq(11) can be rearranged in the standard form of quadratic equation

$$P(|\nabla S|)^2 + Q(|\nabla S|) + R = 0 \tag{14}$$

The solution at a point (i , j) is given as follows

$$|\nabla S|_j^i = \left[\frac{-Q + (Q^2 - 4PR)^{\frac{1}{2}}}{2P}\right]_j^i \tag{15}$$

where details of P, Q, R are given in Jeong(1990).

Differentiation eq(12) for wave direction θ can be written as

$$\theta_j^i = \sin^{-1}\left\{\frac{1}{|\nabla S|_j^i}\left[\tau(|\nabla S|\sin\theta)_{j-1}^{i+1} + (1 - 2\tau)\,(|\nabla S|\sin\theta)_j^{i+1} + \tau(|\nabla S|\sin\theta)_{j+1}^{i+1} - \frac{\Delta x}{2\Delta y}\left\{(|\nabla S|\cos\theta)_{j+1}^i - (|\nabla S|\cos\theta)_{j-1}^i\right\}\right]\right\} \tag{16}$$

Boundary conditions are now discussed to solve the governing equations. Input wave conditions are to be given along the offshore boundary, which are wave height, period and direction. At the side boundaries waves will be transmitted without reflection. Near the land boundary wave will break and be fully absorbed. Wave breaking criteria $H_b = 0.78h_b$ is used for simplicity, where H_b is breaker height and h_b breaker depth.

Initial wave field is defined at all grid points using the Snell's law. For the calculation of wave diffraction we need intermediate values of wave heights and directions over the modelled area. These can be provided from a refraction model based on energy balance equation for the waves propagating on currents(eg. Chae and Song, 1986).

The computation is made row by row and proceeds toward the shoreward direction as in the method for an initial value problem.

As we use steady-wave iteration approach, the simple iterative method for the solution of the equations may have no stability restrictions (Roach, 1982). From the sensitivity analysis for the waves propagating over a circular shoal, variation of computed wave heights is less than 10% for relative grid sizes($L_o/\Delta x$) from 4 to 32 and $L_o/\Delta x = 4$ gives the best fit to the experimental data. It can be said that the grid size of the present model does not significantly depend on wave length. However the restriction is strictly applied to parabolic models. This is one of the major advantages of the present model.

Iterative solution procedure is carried out until the solutions converge to the criterion given as follows

$$\max_{i,j} \left| \frac{(X_j^i)_{new} - (X_j^i)_{old}}{(X_j^i)_{old}} \right| < 0.005 \tag{17}$$

where X_j^i is the computed value at a grid point (i , j). Then the solutions become coupled ones with three governing equations.

The validity and accuracy of the above mentioned numerical scheme have been proved in Chae et al.(1990) through the comparison with experimental data for depth refraction-diffraction problem of monochromatic waves.

Calculation of Wave Spectral Changes

As the present monochromatic wave model is computationally fast and stable especially for short period waves, it may be valuable to simulate spectral transformation of irregular waves propagating in water of complex bathymetry and with ambient currents. Input spectrum $S_o(f, \theta)$ is given as below

$$S_o(f, \theta) = S_o(f)\, G(f, \theta) \tag{18}$$

where

$$S_o(f) = 0.25 H_{1/3}^2\, T_{1/3}(T_{1/3} f)^{-5} \exp[-1.03(T_{1/3} f)^{-4}] \tag{19}$$

is the Bretschneider-Mitsuyasu(B-M hereafter) frequency spectrum, and the directional spreading function $G(f, \theta)$ is given by

$$G(f, \theta) = \left\{\frac{1}{\pi} 2^{2s-1} \frac{\Gamma^2(s+1)}{\Gamma(2s+1)}\right\} \cos^{2s}\left(\frac{\theta}{2}\right) \tag{20}$$

Γ : gamma function

$$s = \begin{cases} S_{max} \cdot (f/f_p)^5 & : f \le f_p \\ S_{max} \cdot (f/f_p)^{-2.5} & : f \ge f_p \end{cases} \tag{21}$$

f_p : Peak frequency of S(f), ($f_p = 1/1.05\ T_{1/3}$ used)

The frequency spectrum and directional spreading function are divided into equal segments. The lower and upper frequency limits of the spectrum are 0.07Hz and 0.37Hz. $\Delta f = 0.02$Hz(15 frequency bins) and $\Delta\theta = 10^o$(17 directional bins) are used.

The input wave amplitude for a particular frequency-directional component is $a_o = [2S_o(f, \theta)\ \Delta f\ \Delta\theta]^{1/2}$. The resulting wave amplitude at any location can be computed using the model, and then the transformed spectrum $S(f, \theta)$ can be obtained as

$$S(f, \theta) = [a/a_o]^2 S_o(f,\theta) \tag{22}$$

Computation Results and Analysis

To demonstrate the applicability of the model numerical computations are made for two cases. The first case is for the refraction-diffraction due to rip-current in a mildly sloping beach as shown in Figure 2(studied by Arthur, 1950).

The computational domain is divided into square grids ($\Delta x = \Delta y = 10$ m) and numerical calculations are performed. Normal incident waves of $H_o = 1$ m, $T = 8$ s are used as an incident wave condition at the offshore boundary. The background(of initial and intermediate) wave field are specified using the Snell's law and the refraction routine in the program, respectively. The dimensionless wave heights H/H_o for two transections are plotted in Figure 3. For the purpose of comparison, parabolic model results(Kirby, 1984) are also shown in the same figure. A comparison of the figures shows that they are in good agreement.

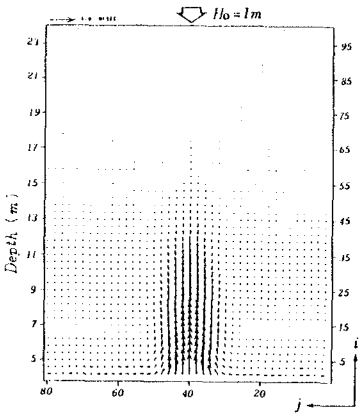

Figure 2. Rip-current field.

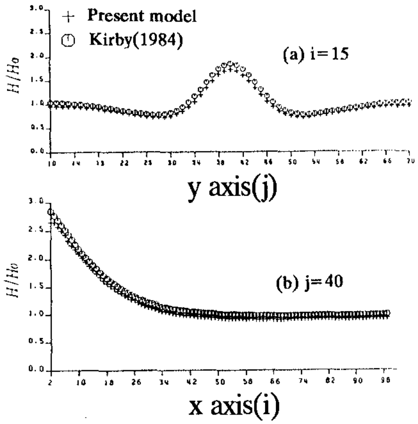

Figure 3. Wave height relative to incident wave for waves interacting with rip current.

The second case is for irregular wave propagation over a shoal as shown in Figure 4, which was recently simulated in a hydraulic laboratory equipped with multi-directional random wave generators(Hiraishi, 1991). The shoal is similar to that used in the experiments of Ito and Tanimoto(1972) with a minimum water depth of 0.05 m at the center of the shoal and constant depth(0.15 m) in the region outside the shoal. B-M spectrum is used for the input spectrum for which $H_{1/3}$ = 0.1 m, $T_{1/3}$ = 1.5 s, and S_{max} = 75(narrow directional spectrum) are used. The grid sizes used are $\Delta x = \Delta y$ =0.1 m. The results are presented in Figure 5, in the form of normalized wave height against the input wave height. The computations agree very well with experimental data which are for the case of non-breaking waves. As the frequency and directional spectra are not available, the comparison for those spectra between computation and experiment can not be made. However, the spectrum can be simulated by linear superposition of monochromatic wave components(eg. Panchang et al, 1990). From those comparisons, the present model appears to be used effectively for the calculation of irregular wave propagation with respects to computation accuracy and time(26 min. with IBM 386 PC).

The present model is used for the analysis of irregular wave transformation due to combined refraction-diffraction while the waves propagate over a circular shoal(Ito and Tanimoto, 1972). The input spectrum is descretized into segments of Δf and $\Delta\theta$. $H_{1/3}$ = 1.0m and $T_{1/3}$= 5.0 s are used for the frequency spectrum(Figure 6) and angular spreading parameter S_{max} = 25 and 75 for the broad and narrow directional spectra, respectively. Current velocity fields are generated using

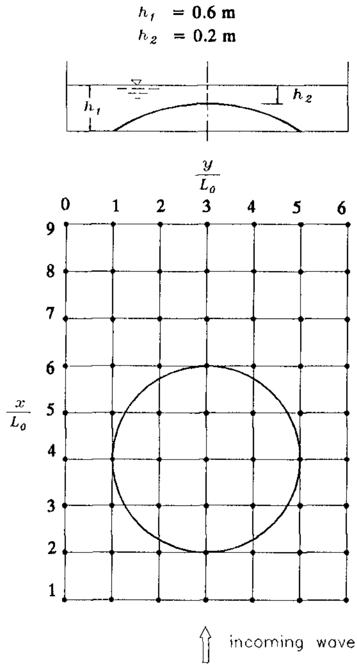

Figure 4. Experimental configuration(Hiraishi, 1991).

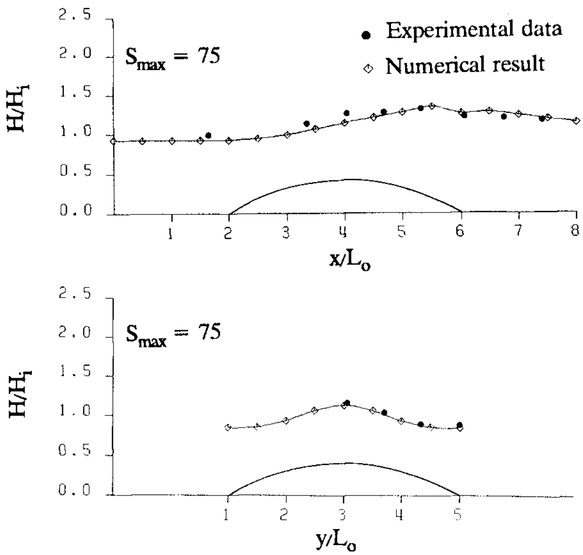

Figure 5. Comparisons between present model results and observed data.

a standard depth-averaged flow model, and assumed frozen during the wave propagation over the field. A uniform current field is assumed at the incoming boundary where the maximum velocity is 0.5 m/s.

The results are shown in Figures 6 and 7. The frequency and frequency-directional spectra are for opposing and following current conditions, and also for broad and narrow directional spreading conditions at a specified point($x/L_o = 7$, $y/L_o = 3$) behind the circular shoal.

As shown in Figure 7, we can clearly see the differences in spectral shapes of input $S_0(f, \theta)$ depending on the value of S_{max}. The smaller value of S_{max} yields less peaky spectral shape and broader band of energy distribution than those with larger S_{max}. When the waves propagate on a current field, the wave height and direction are strongly dependent on the magnitude and direction of the current.

In the following current field the velocities over the shoal are generally larger than those in other region. This will increase the celerity and decrease focusing effect of wave rays propagating over that region, but in the opposing current the effect will be adverse. Such a wave-current interaction causes a large peak around centered direction in the opposing current field and a small peak with side humps in the following current. The waves with directionally narrow banded spectrum will produce very sharp peak, which is contributed mainly from the peak region.

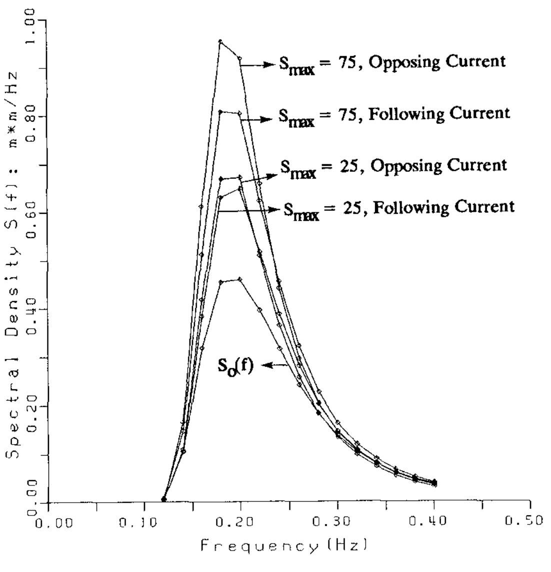

Figure 6. Input frequency spectra($S_0(f)$) and output frequency spectra($S(f)$) at $x/L_o = 7$, $y/L_o = 3$.

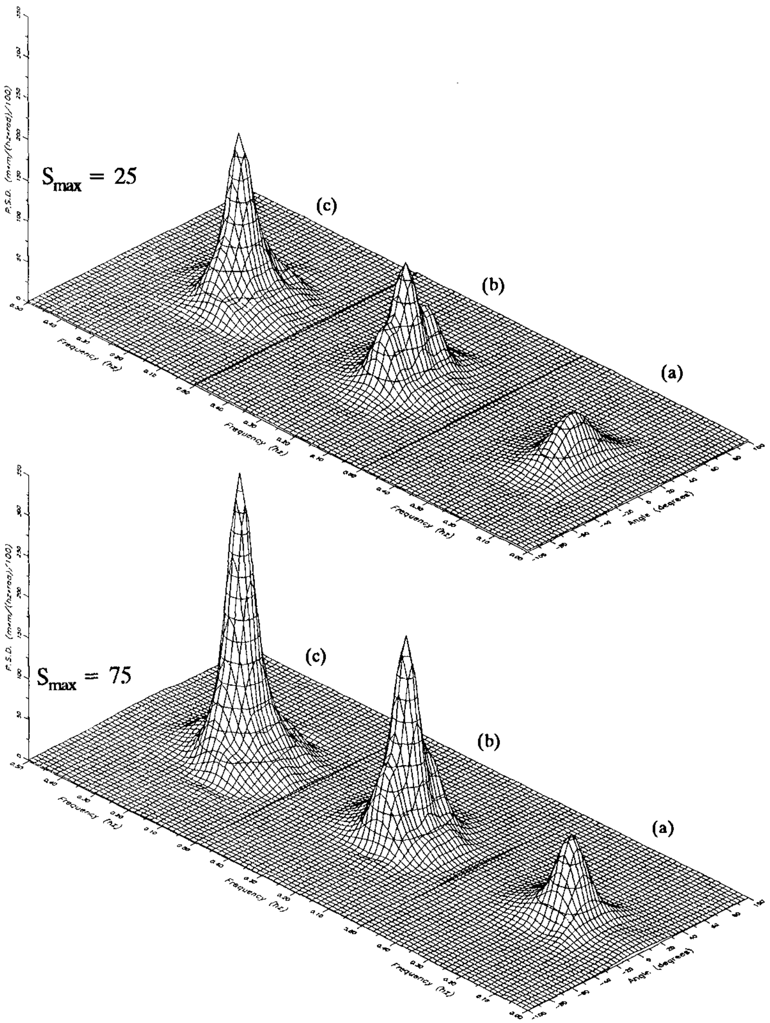

Figure 7. Input directional spectra($S_o(f,\theta)$) and output directional spectra($S(f, \theta)$) at $x/L_o = 7$, $y/L_o = 3$ for different S_{max} and current conditions. (a) $S_o(f,\theta)$, (b) $S(f,\theta)$ with following current, (c) $S(f,\theta)$ with opposing current.

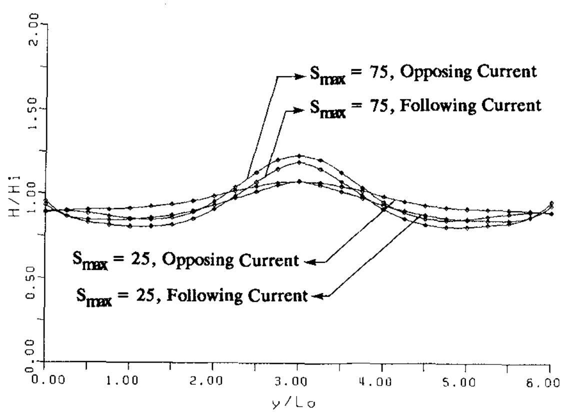

Figure 8. Wave height comparisons, for narrow and broad directional spectra.

The computed frequency spectra are shown in Figure 6. The spectral peaks are almost at the same frequency, the amplification is prominemt in the peak frequency region, where the current effects are also dominant.

The propagation of wave spectra with narrow or broad directional spread shows a little difference between the wave heights in the following and opposing current conditions. The wave heights in the opposing current field are generally larger than those in the following current field(Figure 8).

Conclusions

A set of elliptic type mild-slope equations has been derived for wave-current interactions over a slowly varying topography. Numerical computation method to solve the equations has been presented. The model solves the elliptic equations in a way similar to an initial value problems. Accuracy of numerical computation does not greatly depend on grid size. It can be said that the present model is efficient for wave propagation problems in a large coastal area. Numerical results are shown for transformation of the waves propagating on a rip-current in a mildly sloping beach. They are in good agreement with published ones(Kirby, 1984).

It is also shown that spectral transformation of irregular waves can be satisfactorily simulated by summing up the results from a monochromatic refraction-diffraction model for component waves of a spectrum. From the analysis of frequency-directional spectrum for waves propagating on currents flowing over a mound we can see large differences in spectra depending on current directions, but there is a little difference in wave heights. When the waves propagate on strong currents in shallow water, non-linearity of the waves and wave breaking will be significant, and therefore this model should not be applied.

References

Arthur, R.S.(1950). "Refraction of shallow water waves: the combined effect of currents and underwater topography." Trans. Amer. Geophys. Union, 31(4), 549-552.

Berkhoff, J.C.W.(1972). "Computation of combined refraction-diffraction." Proc. 13th Int. Coast. Engrg. Conf., ASCE, Vancouver, Canada, 471-490.

Booij, N.(1981). "Gravity waves on water with non-uniform depth and current." Report 81-1, Dept. of Civ. Eng. Delft Univ. of Technol., Delft.

Chae, J.W., Jeong, S.T., Yum, K.D., and Song, W.O.(1990). "Current-depth refraction and diffraction model for regular water waves." 7th Congress APD of IAHR, Beijing, China, 357-362.

Chae, J.W., and Song, W.O.(1986). "Current-depth refraction of directional wave spectra." 5th Congress APD of IAHR, Seoul, Korea, 3, 15-34.

Ebersole, B.A.(1985). "Refraction-diffraction model for linear water waves." J. Wtrway. Port, Coast. Oc. Engrg., ASCE, 111(6), 939-953.

Hiraishi, T(1991). "Generation of multi-directional irregular waves and its application." (in personal communication).

Ito, Y., and Tanimoto, K.(1972). "A method of numerical analysis of wave propagation - application to wave diffraction and refraction." Proc. 13th Int. Coast. Engrg. Conf., ASCE, Vancouver, Canada, 503-522.

Jeong, S.T.(1990). "Wave transformations in regions of slowly varying depths with currents." PhD thesis, Dept. of Civil Eng., Seoul National Univ.

Kirby, J.T.(1984). "A note on linear surface wave-current interaction over slowly varying topography." J. Geophys. Res., 89(C1), 745-747.

Liu, P.L.-F.(1983). "Wave-current interactions on a slowly varying topography." J. Geophys. Res., 88(C7), 4421-4426.

Ohnaka, S., Watanabe, A., and Isobe, M.(1988). "Numerical modelling of wave deformation with a current." Proc. 21th Int. Coast. Engrg. Conf., ASCE, 393-407.

Panchang, V.G., Wei, G., Pearce, B.R., and Briggs, M.J.(1990). "Numerical simulation of irregular wave propagation over shoal." J. Wtway., Port, Coast. and Oc. Engrg., 116(3), 324-340.

Roache, P.J.(1982). "Computational fluid dynamics." Hermosa publishers.